



Time-course of *S*-cone system adaptation to simple and complex fields

Arthur G. Shapiro^{a,*}, Jennifer L. Beere^a, Qasim Zaidi^b

^a Department of Psychology, Bucknell University, Lewisburg, PA 17837, USA

^b SUNY College of Optometry, 33 W. 42nd St., New York, NY 10036, USA

Received 18 April 2001; received in revised form 25 June 2002

Abstract

We examine the temporal nature of adaptation at different stages of the *S*-cone color system. All lights were restricted to the *S*-cone-only (a constant *L* and *M*) cardinal axis in color space passing through mid-white (*W*). The observer initially adapted to a steady uniform field with a chromaticity on the $-S$ end of the axis or on the $+S$ end of the axis or a complex field composed of chromaticity $-S$ and $+S$ ($\pm S$ adaptation). The observer then readapted to a steady uniform field of chromaticity *W* for a variable length of time (i.e., 0, 0.1, 0.25, 0.5, 1.0, or 2.0 s). A probe-flash technique was used to measure *S*-cone discrimination at various points along the *S*-cone-only cardinal axis. This allowed estimation of the response of the *S*-cone system over an extended response range. Following exposure to the $-S$ and $+S$ uniform fields, sensitivity was maximal at or near the chromaticity of the initial adaptation field and decreased linearly away from the adapting point. The shift from $+S$ to *W* occurred more rapidly than the shift from $-S$ to *W*; both of these shifts can be described by a multiplicative scaling of the *S*-cone signal. Following $\pm S$ adaptation the threshold curve initially had a shape similar to that measured following $-S$ adaptation, but returned rapidly to the *W* adaptation state. The shift following $\pm S$ adaptation cannot be described by the multiplicative model, but can be explained by a change in the shape of the non-linearity. The results suggest the existence of fast post-receptoral processes.

© 2003 Published by Elsevier Science Ltd.

1. Introduction

We examine the temporal nature of adaptation at different stages of color processing. Current models of color vision posit two post-receptoral cardinal mechanisms preferentially tuned to the *S* and the *L–M* cardinal axes (Krauskopf, Williams, & Heeley, 1982); there is also evidence for higher-order color mechanisms tuned to intermediate color angles (Krauskopf, Zaidi, & Mandler, 1986; Webster & Mollon, 1991; Webster & Mollon, 1994). Each of these parallel systems has unique processing characteristics. In this paper, we restrict our analysis to adaptation in the *S*-cone system in order to take advantage of previous models describing adaptation to uniform fields in the *S*-cone system. Shapiro, Baldwin, and Zaidi (2002) presented an analysis similar to the one shown here for the *L–M* system.

Zaidi, Shapiro, and Hood (1992) developed a model that describes shifts in *S*-cone response following ad-

aptation to spatially uniform steady fields that differed in *S*-cone excitation. In this study, we expand upon this model by measuring the time-course for adaptation to one background after adapting to another. As with Zaidi, Shapiro, and Hood, we measured sensitivity to lights limited to an equiluminant tritan confusion line through a neutral white (i.e., the constant *L* & *M* axis of (Derrington, Krauskopf, & Lennie, 1984; Krauskopf et al., 1982)). To examine adaptation processes at different levels of the system, we compared the response while adapting to spatially uniform steady fields (Zaidi et al., 1992) to the response measured following adaptation to fields modulated in time and space (Shapiro & Zaidi, 1992; Zaidi & Shapiro, 1993; Zaidi, Spehar, & DeBonet, 1998). To separate the effects of time-dependent adaptation processes from those of static response non-linearities, we used a modification of the probe-flash technique that allowed response functions to be measured over an extended range of inputs at transitory and steady adaptation states (Shapiro, Beere, & Zaidi, 2000).

We assume that the *S*-cone color system is composed of the difference between *S*-cone outputs and the sum of the *L*- and *M*-cone outputs. This system will respond to

* Corresponding author.

E-mail address: shapiro@bucknell.edu (A.G. Shapiro).

modulation along the S cardinal axis of Derrington et al. (1984), but not to modulation in the plane formed by the other two cardinal axes. Zaidi et al. (1992) showed that at mid-white, the S and $L + M$ components were balanced at the site of opponent combination. This system is not the same as the non-linear “yellow–blue” hue system of Herring (1878), which is defined in terms of null responses to “unique-red” and “unique-green” colors (Burns, Elsner, Pokorny, & Smith, 1984; Ikeda & Ayama, 1980; Larimer, Krantz, & Cicerone, 1975).

A comprehensive characterization of the S -cone color system in any adaptation state requires discrimination measurements across an extended response range. Such measurements can be made with a probe–flash technique, which consists of adapting, flashed, and probe lights (Geisler, 1978; Hayhoe, Benimoff, & Hood, 1987). At every adaptation state, the observer is asked to discriminate the probes from the flashes. The flashed lights can differ from the adapting light, and flash and probe are presented too briefly to alter the adaptation state. This method separates sensitivity differences within an adaptation state from sensitivity changes across adaptation states. Zaidi et al. (1992) used this method for the isolated S -cone color mechanisms, and Shapiro, Zaidi, and Hood (1990) did so for the isolated $L–M$ mechanism. Other investigators have used analogous methods (Krauskopf & Gegenfurtner, 1992; Pokorny & Smith, 1997; Yeh, Pokorny, & Smith, 1993). Probe–flash methods were extended for measuring the time-course of light adaptation processes (Hayhoe et al., 1987), and adaptation to theoretically defined color lines (Shapiro et al., 2000).

For adaptation to steady spatially uniform fields along the tritan axis, Zaidi et al. (1992) showed that maximal sensitivity is limited to a small range of inputs in any state of adaptation and that adaptation shifts the range of maximal sensitivity to coincide with the steady stimulus. Similar results were found by Krauskopf and Gegenfurtner (1992) and Yeh et al. (1993). These and other experimental results on the S -cone system were fit well by a model that included identical multiplicative gain control mechanisms in the S and $L + M$ pre-opponent branches, and a post-opponent static sigmoidal non-linearity with a greater amount of compression for $S > L + M$ than for $S < L + M$ inputs. In this paper we first replicated the extreme steady state conditions of Zaidi et al. (1992) and fit the model to estimate parameters for the individual observers. We then made measurements at various times during the shift between the steady adaptation states, and tested whether the same model can fit the data while allowing the effective adaptation state to vary as a linear combination of the two steady states.

The empirical results above are consistent with Craik’s (1938) notion of efficiency: that when adapted to a certain level, an observer’s discrimination should be

best at that level. This property would be functionally optimal if it could be assumed that the frequency distribution of stimulation in any state has a maximum at or near the adapting level. The situation is quite different when an observer is viewing a spatially variegated field with the use of eye movements, thus exposing each point on the retina to a range of colors different from the average of the field. It would be more efficient to adapt the range of sensitivity to the range of expected stimulation, and trends in this direction have been found after prolonged exposure to temporal modulation (Shapiro & Zaidi, 1992; Zaidi & Shapiro, 1993) and to spatial variation (Zaidi et al., 1998). After such spatially or temporally complex stimulation, the change in sensitivity could not be explained by conventional multiplicative or subtractive adaptation combined with an invariant response non-linearity, but instead required a change in the shape of the response function. Adaptation to complex fields thus requires qualitatively different processes than adaptation to steady uniform fields.

2. Methods

The techniques and equipment common to all experiments are described in this section. The unique features and parametric conditions for each experiment are given with the results in Section 3.

2.1. Equipment

The stimuli were generated with a Cambridge Research VSG 2/3 graphics board and displayed on a Radius Press View monitor. The Cambridge Research OptiCal system was used for luminance calibration and gamma correction. The measurements were checked with a Photoresearch 650 spectroradiometer.

2.2. Observers

Three color-normal observers (two female, one male) participated in this study; one is the second author of this manuscript. Equiluminance of the S axis was set for each observer using a flicker photometric procedure. Within the range of the phosphors no observer differed substantially from the standard observer.

2.3. Stimulus space

All lights fell along an S -only ($S/L + M$) axis through a neutral white (MacLeod & Boynton, 1979). This axis, depicted in Fig. 1, is referred to as the S cardinal axis; $-S$ and $+S$ are the chromaticities on the extreme ends of this line. The chromaticity coordinates of the $-S$, W , and $+S$ points in MacLeod and Boynton (1979) units are (0.005, 0.635), (0.017, 0.635) and (0.029, 0.635). As in

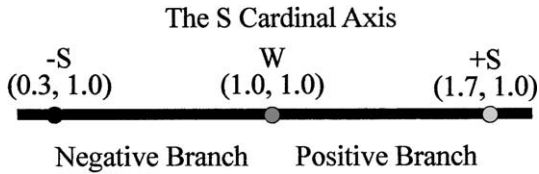


Fig. 1. *S* cardinal axis passing through mid-white (*W*). All lights in the experiment were restricted to the *S* axis of a MacLeod and Boynton (1979) chromaticity diagram. The end points of the line, labeled $-S$ and $+S$, had a MacLeod–Boynton chromaticity of (0.005, 0.635) and (0.029, 0.635). Following Zaidi et al. (1992), we normalized the lights so that *W* would equal (1,1). The normalized chromaticity units are shown in parentheses.

Zaidi et al. (1992) we normalize the units in Fig. 1 so that *W* is equal to (1,1). We frequently distinguish between the lights on opposite sides of *W*. The portion between $-S$ and *W* is referred to as the negative branch; between *W* and $+S$, as the positive branch. The luminance was held constant at 50 cd/m², and was high enough to alleviate concerns about rod-system mediation of detection thresholds (Shapiro, Pokorny, & Smith, 1996).

2.4. Procedure

Fig. 2A shows the spatial configuration and temporal sequence for the experimental stimulus. The procedure

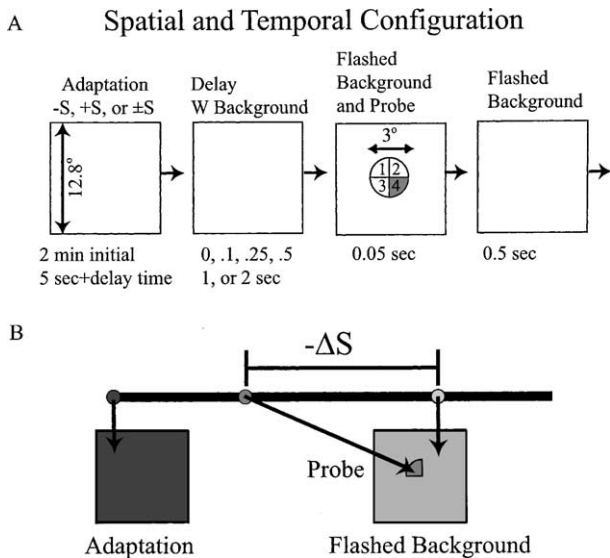


Fig. 2. (A) The spatial configuration and temporal sequence of the stimulus. The observer adapted to either a uniform field with chromaticity $-S$, *W*, or $+S$ or a complex field ($\pm S$). A field of chromaticity *W* was presented for a variable duration between the offset of the adapting stimulus and the presentation of the flash–probe combination. The observer’s task was to identify which quadrant differed in chromaticity from the flashed background. (B) Thresholds were measured for the distance between the test light and flashed background along the *S* axis.

was designed to measure the sensitivity of the *S*-cone system over an extended range of inputs; i.e., the observer adapted to a field of a particular chromaticity, and thresholds were measured at a number of points along the *S* axis. The observer began the experiment by fixating at a spot in the center of a 12.8-degree square adaptation field. The field was set to an initial adaptation chromaticity on the *S* line: $-S$, *W*, $+S$, or a spatially and temporally complex adapting stimulus ($\pm S$). After a 120-s adaptation period, the field switched to the second adaptation chromaticity (*W*) for a fixed adaptation period (0.0, 0.1, 0.25, 0.5, 1.0, or 2.0 s). The chromaticity of the field was then changed to that of the flash, with a probe superimposed in the center. The probe–flash combination remained for 0.05 s. To remove the effects of positive afterimages, the flash remained for an additional 0.5 s after the probe disappeared (Geisler, 1978). The initial adaptation chromaticity was then presented for a 5-s “top-up” adaptation period.

The probe was configured as four quadrants of a 3 degree disk. The observer’s 4-alternative forced-choice (4AFC) task was to identify the location quadrant of the probe by pressing the corresponding button on a response box. Flashes were distributed at up to 11 evenly spaced judgment points along the *S*-cone axis (Fig. 2B) The probe was always to the $-S$ side of the flash. Difference thresholds were measured at the same judgment points for all adaptation conditions; therefore, threshold changes reflect differences only in the adapting field and the duration of the adaptation interval.

Thresholds were measured by a 2-up/1-down adaptive staircase procedure varying the $-S$ distance between the flash and probe. The staircase stopped after 10 reversals. The difference threshold equaled the mean of the last eight reversals (Wetherill & Levitt, 1965).

3. Results

3.1. Steady-state adaptation model

Fig. 3A–C show threshold curves following adaptation to each of the three different uniform backgrounds, $-S$, *W*, and $+S$ for three observers. The experiment replicates three of the conditions used in Zaidi et al. (1992), and Shapiro and Zaidi (1992). The results were used to estimate the parameters of the model discussed below. Following *W* adaptation (open circles), the difference-threshold is minimum at *W* and increases sharply on the positive branch (the slope of the regression line equals 0.34 for observer JLB, 0.31 for observer LAB, and 0.26 for observer MPP), and less steeply on the negative branch (slope equals -0.04 for observer JLB, -0.19 for observer LAB, and -0.03 for observer MPP). Following $-S$ adaptation (filled circles), thresholds

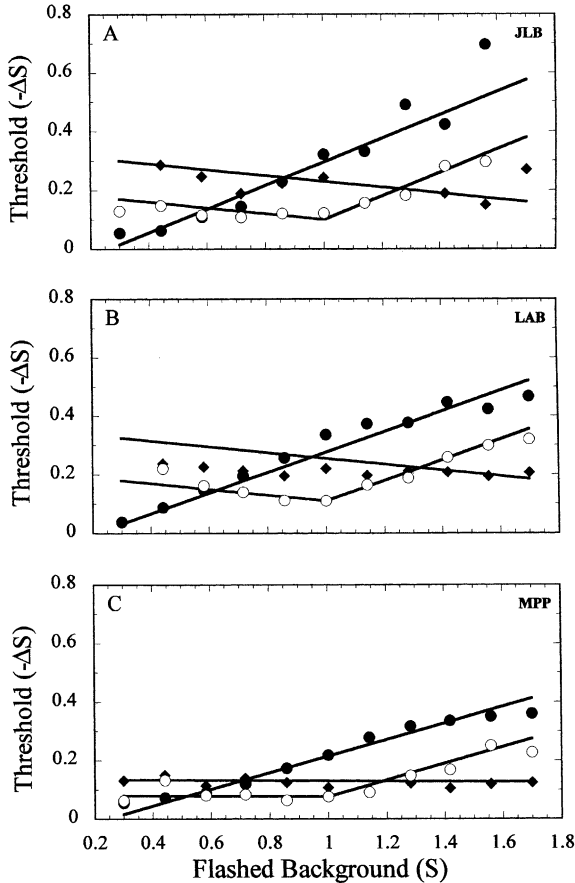


Fig. 3. (A) Threshold curves following adaptation to each of the three uniform backgrounds, $-S$, W , and $+S$. The experiment replicates three of the conditions used in Zaidi et al. (1992), and Shapiro and Zaidi (1992). The lines show the fit of the Zaidi et al. (1992) model. (B) and (C) are the results for the second and third observers.

are minimum at $-S$ and increase linearly with a slope similar to that found on the positive branch of the W adaptation curve (slope equals 0.43 for observer JLB, 0.32 for observer LAB, and 0.24 for MPP). Following $+S$ adaptation (diamonds), thresholds are minimum near $+S$ and increase toward W (slope equals -0.04 for observer JLB, -0.02 for observer LAB, and -0.02 for observer MPP). For both JLB and MPP the slopes on the negative branch are about the same following W and $+S$ adaptation; however, for observer LAB, the slope following $+S$ adaptation was shallower than after W adaptation.

The Zaidi, Shapiro, and Hood model of S -cone system adaptation is depicted in Fig. 4. In this model an opponent signal, $\kappa_S S - \kappa_{LM} (L + M)$, is passed through a compressive response function, R . The values of the gain coefficients, κ_S and κ_{LM} , are set from the S and $L + M$ values of the uniform adaptation background, A_S and A_{LM} . The value of κ_{LM} remained fixed because the experimental variations in this study were limited to the S -cone line.

Model of S-cone System for Uniform Adaptation Lights

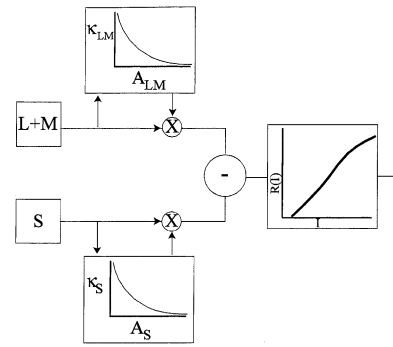


Fig. 4. Graphical description of the Zaidi et al. (1992) model. An opponent signal, $\kappa_S S - \kappa_{LM} (L + M)$, is passed through a compressive response function, R . The values of the gain coefficients, κ_S and κ_{LM} , are set by the S and $L + M$ values of the uniform adaptation background. The value of κ_{LM} remained constant because the experimental variations were limited to the S -cone line. The non-linear response function is the same as that used by Shapiro and Zaidi (1992).

The different slopes on either side of W (Fig. 3) are consistent with previous results (Krauskopf & Gegenfurtner, 1992; Yeh et al., 1993; Zaidi et al., 1992) and suggest an asymmetric non-linear response function. The model incorporates this property as a combination of two logarithmic response functions, $R(I)$, where I is the initial opponent signal:

$$R(I) = \frac{1}{\beta_P} \ln(\alpha + \beta_P(I)) - \frac{1}{\beta_P} \ln(\alpha), \quad \text{if } I \geq 0$$

$$\text{and } R(I) = \frac{1}{\beta_N} \ln(\alpha + \beta_N(I)) - \frac{1}{\beta_N} \ln(\alpha), \quad \text{if } I < 0$$
(1)

α , β_P , and β_N are parameters describing the response non-linearity. We assume that the probability of discriminating between the flashed background (F-P) and the background with the probe (F) is proportional to $R(F) - R(F-P)$ and thus generates a psychometric curve that monotonically increases with probe magnitude. For analytic convenience this probability was approximated by the slope of the response function at the level corresponding to the magnitude of the flashed background, F , multiplied by the magnitude of the probe, P (von Wiegand, Hood, & Graham, 1995; Zaidi & Shapiro, 1993). Eq. (1) predicts straight lines when thresholds are plotted versus judgment chromaticity. A bend at the W point occurs when the flash-probe combination shifts from one non-linearity to the other.

The fit of the model to all three thresholds is shown as solid lines in Fig. 3. Following W adaptation, thresholds on either side of W rise linearly with a slope of β_P for the positive branch and β_N for the negative branch. We therefore estimated β_N and β_P to be equal to the slopes of the regression lines fit to the threshold curves. Similarly, the model predicts that following W adaptation

the thresholds measured from a W background will equal α , the intercept of the regression line. In theory, there can be two estimates of α , one for the positive branch and one for the negative branch. In practice, the difference between these two estimates of α was well within experimental error. The model does well for observers JLB and MPP, and for the positive branch for observer LAB, but not for observer LAB on the negative branch, due to the difference in this observer's slopes following W adaptation and $+S$ adaptation.

3.2. Time-course of adaptation to uniform fields

We measured threshold curves at various intervals during the shift in adaptation from $+S$ to W and from $-S$ to W . The purpose was to estimate the response of the S -cone system during the shift in adaptation. We considered whether the effects of adaptation can be adequately modeled by changes in the parameter κ_S as a function of the time-integrated S -cone level.

3.2.1. Procedure

The observer initially adapted to a $+S$ or $-S$ background. Before the presentation of the probe-flash combination, a field with a chromaticity of W was presented for 0.0, 0.1, 0.25, 0.5, 1.0, or 2.0 s (adaptation interval). Probe-flash threshold curves were measured after adaptation to W for these time intervals. All other procedures were the same as in the first experiment.

3.2.2. Results

In Figs. 5–7 the filled diamonds show threshold curves following $+S$ adaptation measured for various intervals of W adaptation. As a baseline, the open circles show thresholds measured following uniform W adaptation, re-plotted from Fig. 3. The top panel shows the threshold curves from the 0 s delay condition, re-plotted from Fig. 3. For all three observers the threshold curve is relatively flat. As the W adaptation interval increases, shown by successive panels, the threshold curves shift toward that measured under steady W adaptation. The shift from steady $+S$ to steady W adaptation was nearly complete within 0.1 s for all three observers.

The filled circles in Figs. 8–10 show threshold curves for similar intervals of W adaptation following $-S$ adaptation. The top panel shows the steady adaptation conditions re-plotted from Fig. 3. For all three observers, the recovery response was slower than it was after $+S$ adaptation. For observer JLB, the minimum threshold remained at $-S$ until about 0.5 s, and adaptation was not complete at 2 s. Observers LAB and MPP had faster recovery times, and adaptation was complete within 1.0 s; this was still appreciably longer than recovery after $+S$ adaptation.

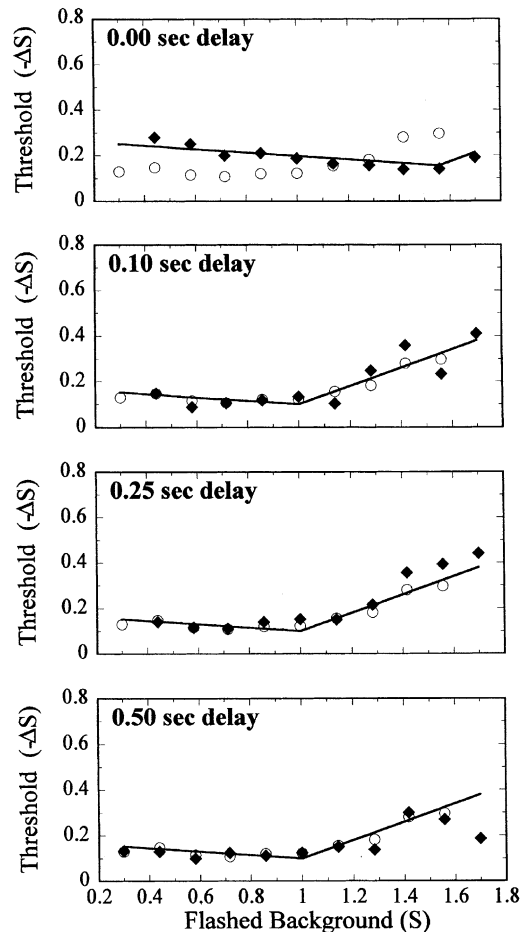


Fig. 5. The threshold curves following $+S$ adaptation for observer JLB (filled diamonds). The open circles are the threshold curves following W adaptation (from Fig. 3). Each successive panel shows an increase in the delay duration. The solid line shows the fit of the model assuming that the shift from the $+S$ background to W only affects the gain of the S -cone branch (i.e., a change in the parameter κ_S).

3.2.3. Multiplicative gain control model applied to the time-course data

The solid lines in Figs. 5–10 represent the best fit of the model, where the values of the parameters α , β_N , and β_P were estimated solely from the threshold curves in Fig. 3. The parameter κ_S was adjusted in each panel to minimize the least-squared error. As can be seen in all panels, the model describes the threshold curves reasonably well. As reported above, observer LAB's slope on the negative branch in the W adaptation condition was different from the slope in the $+S$ adaptation condition. To capture both the beginning and ending adaptation states for this observer, the requirement that the slope of the curve be fixed from the W data was relaxed for this condition; the value β_N was between that estimated from W adaptation condition and from the $+S$ adaptation condition in which the delay equals 0 s.

The value of κ_S versus time, as shown in the model, can be estimated directly from the data. This in turn can

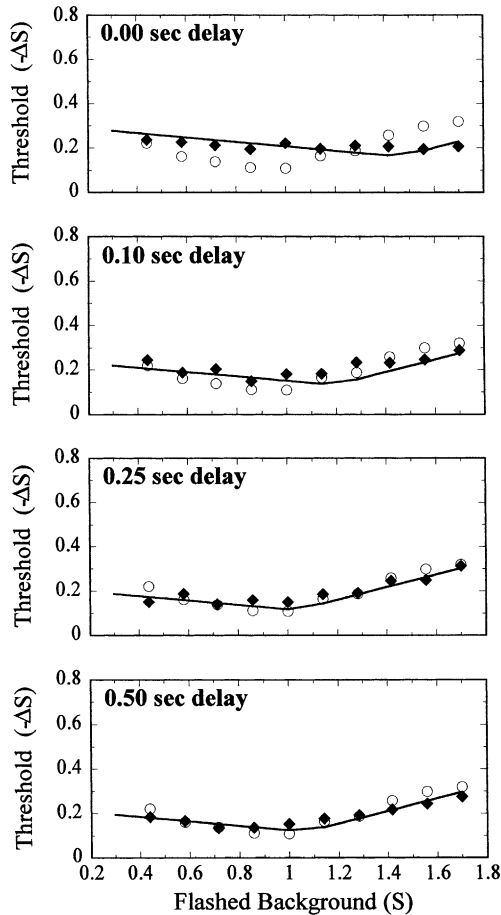


Fig. 6. Same conditions as Fig. 5 for observer LAB.

be used to calculate the value of $\gamma(t)$, the proportion of completed adaptation at time t :

$$\gamma(t) = (A_{\kappa(t)} - A_0) / (A_w - A_0) \quad (2)$$

$A_{\kappa(t)}$ is the effective adaptation state, directly calculated from the estimated value of $\kappa_S(t)$; A_0 is the adaptation signal from the adapting background at time 0 (i.e., for $+S$ adaptation $A_0 = 1.7$, and for $-S$ adaptation $A_0 = 0.3$); and A_w is the adaptation at the end state (this value is always equal to 1). When γ equals 0 the adaptation level is equal to the adapting background; when γ equals 1 adaptation has returned to W .

Fig. 11 plots γ as a function of time following $+S$ adaptation (diamonds) and following $-S$ adaptation (circles). For all conditions γ starts near 0, and then increases towards 1. The change in γ following $+S$ adaptation is faster than the change following $-S$ adaptation. For observer JLB, γ following $-S$ adaptation remained relatively constant for the first 0.5 s. For observer LAB the γ for $-S$ adaptation increases to a value of 1 more gradually than for the other two observers. The gradual change (as well as the high initial value of γ)

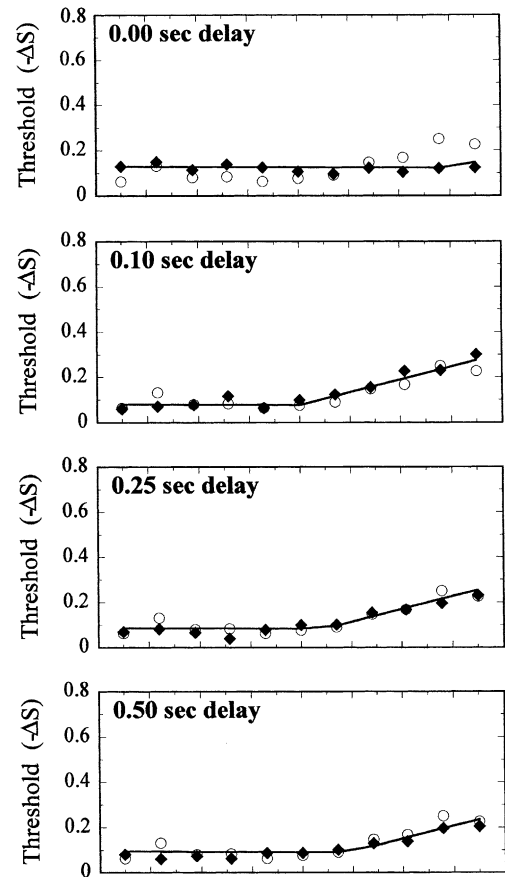


Fig. 7. Same conditions as Fig. 5 for observer MPP.

is related to the removal of one of the modeling restrictions for this observer as discussed above. The removal of the restrictions would not affect the value of γ for the other two observers. Nonetheless, even for observer LAB, the value of γ rises faster following $+S$ adaptation than following $-S$ adaptation.

3.3. The time-course of adaptation to W following $\pm S$ adaptation

A complex field composed of randomly alternating $-S$ and $+S$ squares produces the same space- and time-averaged luminance as W . In principle, this stimulus is similar to the temporally modulated habituation stimulus used by a number of previous researchers (Krauskopf et al., 1982; Shapiro & Zaidi, 1992; Webster & Mollon, 1994). Mechanisms that enable the visual system to adapt to such lights arise beyond the level of the photoreceptors. Krauskopf et al. showed that even though modulation along a luminance axis creates greater cone-level excitation than $L-M$ modulation, prolonged $L-M$ modulation elevated $L-M$ thresholds, but prolonged luminance modulation did not. Shapiro and Zaidi (1992) showed that probe-flash threshold

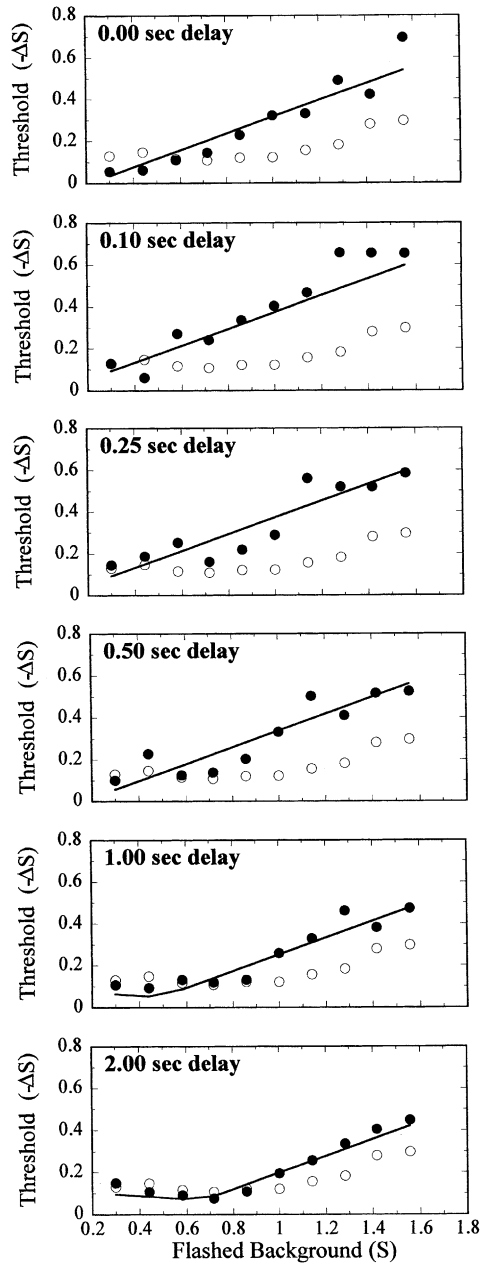


Fig. 8. Threshold curves following $-S$ adaptation for observer JLB (filled circles). The open circles are the threshold curves following W adaptation (from Fig. 3). Each successive panel shows an increase in the delay duration. The solid line shows the fit of the model assuming that the shift from the $-S$ background to W only affects the gain of the S -cone branch (i.e., a change in the parameter κ_S).

curves measured after prolonged temporal modulation were qualitatively different from those curves measured after adaptation to steady uniform fields.

The visual system could conceivably adapt to spatially and temporally complex lights in a number of ways: (1) The visual system could adapt to the average chromaticity of the stimulus. Such adaptation would result in a 'v' shaped threshold curve centered at W (similar to the open circles in Fig. 3). (2) The visual system could adapt

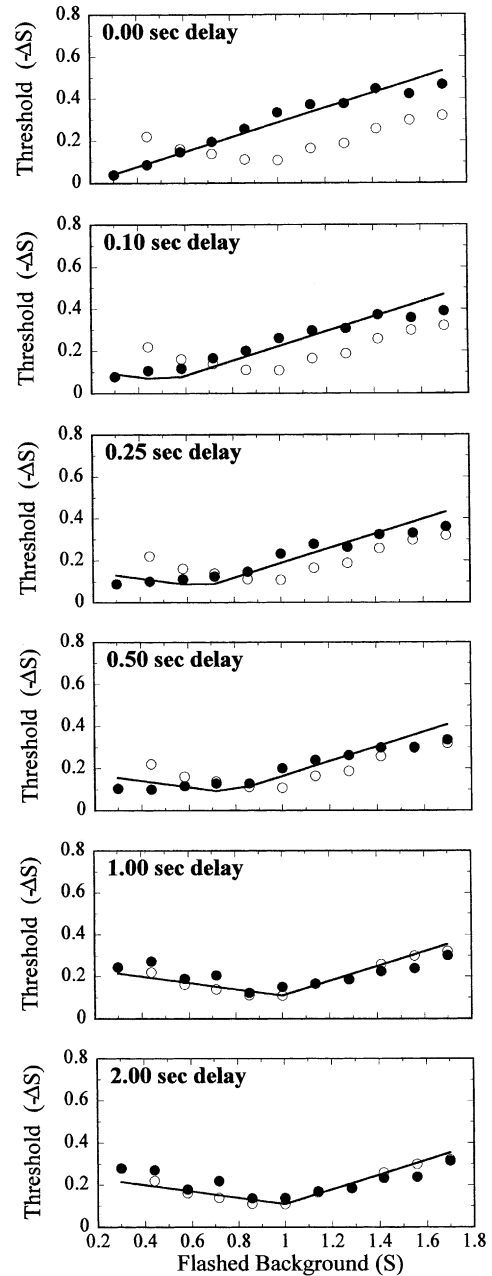


Fig. 9. Same conditions as Fig. 8 for observer LAB.

independently to the $-S$ and $+S$ chromaticities; i.e., there may be two independent detection mechanisms maximally sensitive to either $-S$ or $+S$. The threshold curve would be an inverted "v" formed by the minima of the triangles and filled circles in Fig. 3. (3) There could be a post-opponent multiplicative gain change after the response non-linearity. Shapiro and Zaidi (1992) showed algebraically that this would produce threshold curves that are steeper than those during W adaptation and that retain a minimum at W . (4) There could be a multiplicative gain change after the opponent combination but before the response non-linearity. Shapiro and Zaidi (1992) showed that this would produce a

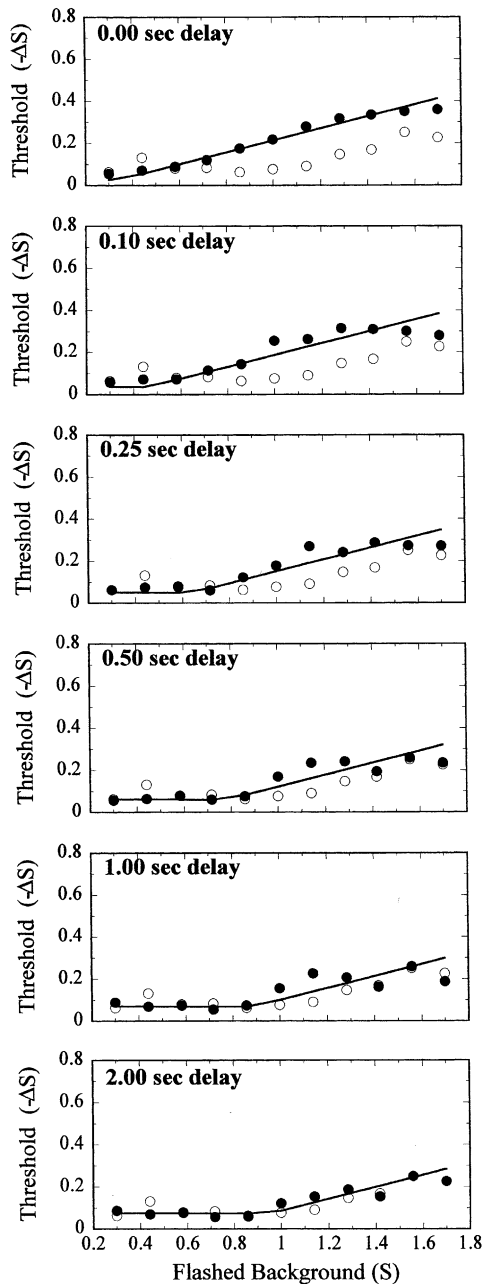


Fig. 10. Same conditions as Fig. 8 for observer MPP.

parallel elevation of each branch of the threshold curve. (5) The visual system could adjust its response to represent the statistical distribution of the chromaticities in a manner akin to response equalization (Zaidi & Shapiro, 1993; Zaidi et al., 1998).

Shapiro and Zaidi (1992) showed that for sinusoidally modulated habituation stimuli, the threshold curves could not be described by a multiplicative gain control placed before or after the non-linearity. Similar conclusions were reached by Zaidi et al. (1998) for adaptation to spatially complex fields. The thresholds could best be described by a change in shape of the non-

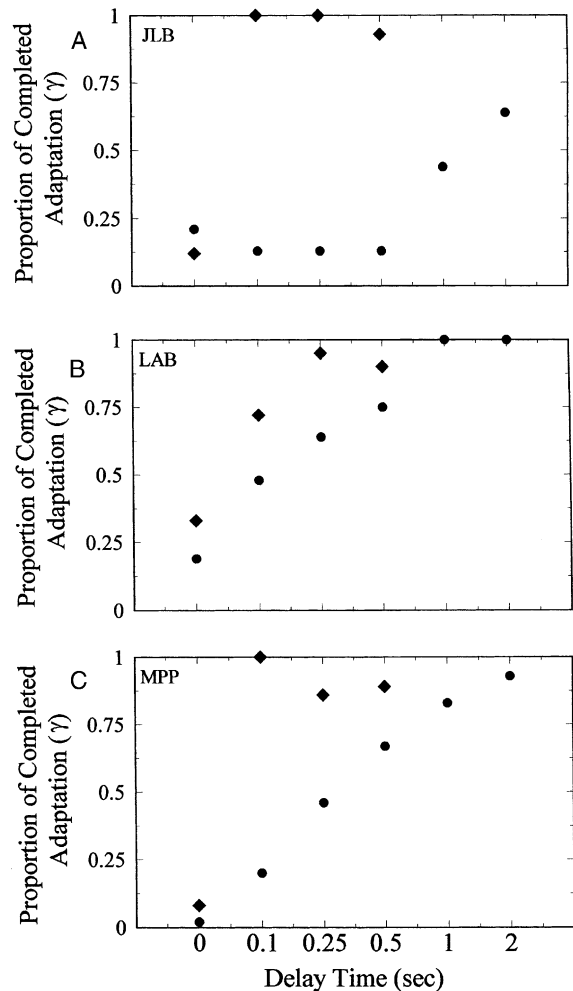


Fig. 11. (A) The proportion of completed adaptation, γ , over time following uniform $+S$ adaptation (diamonds) and uniform $-S$ adaptation (circles) for observer JLB. γ is a transformation of κ_S . See text for details. (B) Observer LAB. (C) Observer MPP.

linearity (i.e., model 5). The post-habituation response function was more linear than the response function before habituation. In this experiment we extended the paradigm to investigate the time-course of the response change to a combination of spatial and temporal modulation.

3.3.1. Adapting stimulus

A depiction of the $\pm S$ adapting stimulus is shown in Fig. 12. The field was composed of 3.7 squares per degree of visual angle. The size of the squares was set to maximize threshold elevation based on measurements of checkerboard adaptation (Zaidi et al., 1998). The chromaticity of each square was either $-S$ or $+S$ and was randomly reassigned every 0.1 s. The space- and time-averaged chromaticity of the field was W ; i.e., every frame had the same number of $-S$ and $+S$ pixels. A random process determined the chromaticity for each

The $\pm S$ adaptation stimulus

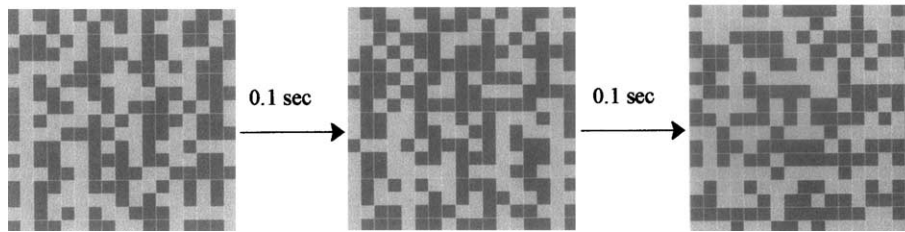


Fig. 12. A depiction of the stimulus for $\pm S$ adaptation. The field was composed of 3.7 squares per degree of visual angle. The chromaticity of each square was either $-S$ or $+S$ and was randomly reassigned every 0.1 s. The space- and time-averaged chromaticity was equal to W .

square. Because of the length of the trials the time-average did not differ substantially from W . On average $P(-S) = P(+S) = 0.5$, where $P(-S)$ and $P(+S)$ equaled the proportion that a pixel was set to $-S$ or to $+S$.

3.3.2. Procedure

The procedure was the same as in Experiment 1, except that the observer adapted to the $\pm S$ stimulus instead of the uniform $-S$ or $+S$ field. Probe-flash threshold curves were measured for various intervals of re-adaptation to W .

3.3.3. Results

The filled circles in Figs. 13–15 show the time course of recovery from $\pm S$ adaptation for each observer. The open circles show the threshold values after steady adaptation to W . The threshold curve measured directly after $\pm S$ adaptation (0.0 s condition) has a similar shape to that measured following steady $-S$ adaptation, i.e., a straight line increasing from the $-S$ chromaticity. The dashed lines show the fit of the model to the $-S$ adaptation condition; the lines are included to make comparisons between $-S$ and $\pm S$ adaptation. For all three observers, thresholds are elevated more following $\pm S$ adaptation than following $-S$ adaptation, and thus could not be explained by any early non-linearity that biases the average $\pm S$ adaptation towards $-S$ or $+S$. Observer LAB never returned to the initial state, but there was little change between 0.5 and 1.0 s.

3.3.4. Change in shape of non-linearity

The solid lines in Figs. 11–13 are the predictions of a model originally suggested by Shapiro and Zaidi (1992), in which $\pm S$ adaptation increases the range of linear response. An increase in the linear range occurs when the value of α is increased and the absolute values of β_P and β_N are decreased. The changes in parameters shown for these data were consistent with a change in the shape of the response function that diminishes within 0.5 s.

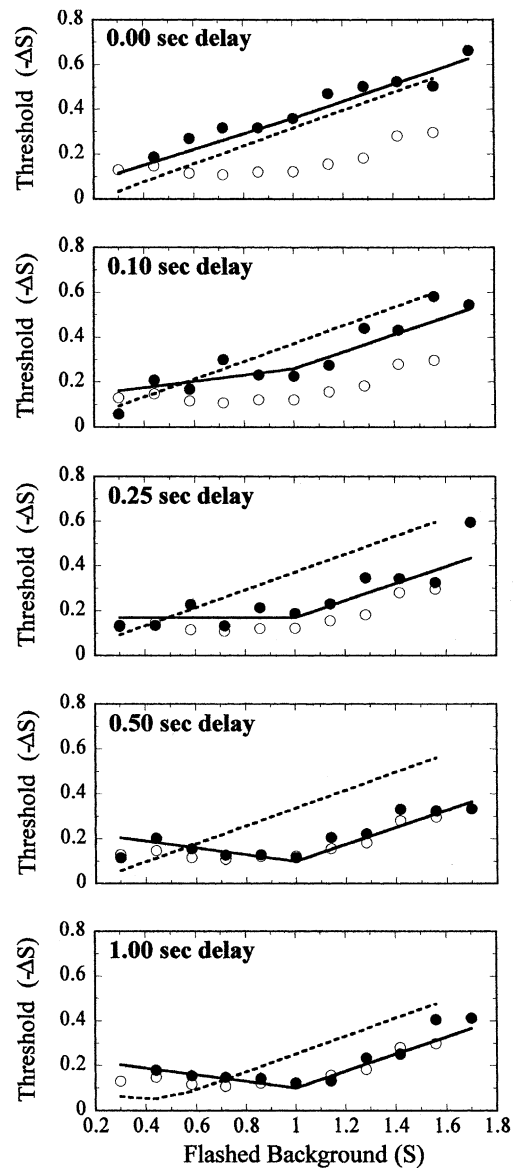


Fig. 13. Threshold curves following $\pm S$ adaptation for observer JLB (filled circles). The open circles are the threshold curves following W adaptation (from Fig. 3). Each successive panel shows an increase in the delay duration. The solid line shows a fit of the model, allowing for a change in the shape of the non-linearity, as proposed by Shapiro and Zaidi (1992). The dashed line shows the model fit to the $-S$ adaptation data from Fig. 8.

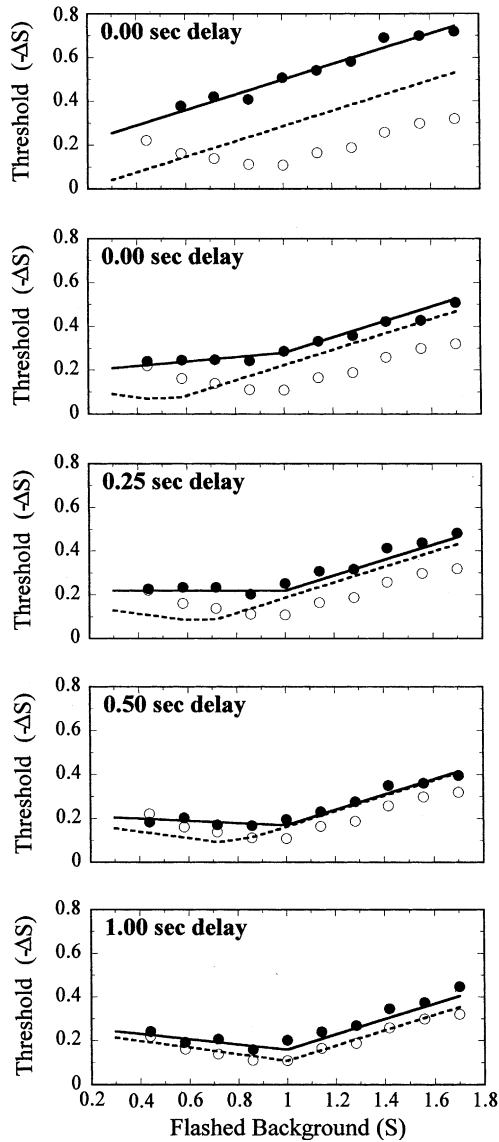


Fig. 14. Same conditions as Fig. 13 for observer LAB. The dashed line shows the model fit to the $-S$ adaptation data from Fig. 9.

4. Discussion

The results of this study help to define the nature of detection and adaptation mechanisms in the S -cone system. Separate mechanisms for detecting $+\Delta S$ and $-\Delta S$ from the adapting level were originally proposed because the two types of thresholds were selectively elevated after the observer adapted to saw-tooth waveforms (Krauskopf et al., 1986), and because thresholds for discriminating between purely temporal color changes were approximately proportional to the cosine of the color angle between them (Zaidi & Halevy, 1993). Such “rectified” mechanisms have also been invoked to explain results on color induction (Krauskopf et al., 1986; Pokorny & Smith, 1997) and differences in

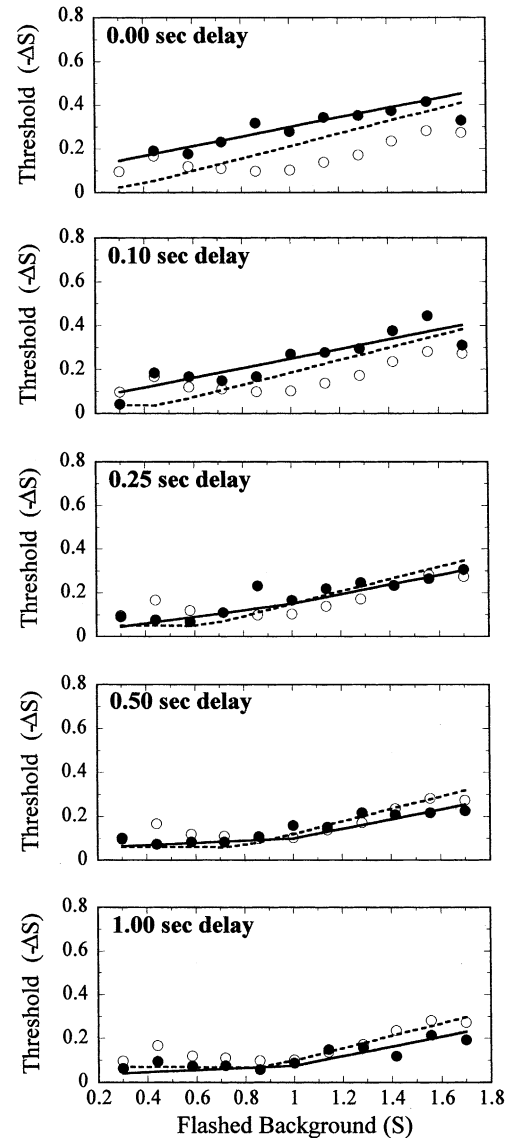


Fig. 15. Same conditions as Fig. 13 for observer MPP. The dashed line shows the model fit to the $-S$ adaptation data from Fig. 10.

the detection of $-S$ and $+S$ excursions (McLellan & Eskew, 2000).

Physiological evidence has been presented for a Blue-on pathway mediated by the small bistratified ganglion cells and a separate Blue-off pathway presumably mediated by a subclass of midget ganglion cells (Dacey, 2000). The bistratified ganglion cells form connections with cells in koniocellular layers in the lateral geniculate nucleus (LGN), and these cells connect directly with cytochrome-oxidase blobs in the primary visual cortex (Hendry & Reid, 2000). The existence of a Blue-off pathway has been well documented (Valberg, Lee, & Tigwell, 1986). The pathway of the Blue-off cells has not yet been identified but presumably remains separate from the Blue-on pathway at least until the level of the LGN.

A comparison of the behavior of the positive branch versus the negative branch in a number of the conditions supports the notion that these two branches are served by separate mechanisms. The mechanism whose response we are estimating appears to be determined by the sign of the judgment chromaticity relative to the effective adapting chromaticity (as compared to the adapting light, or the direction of the probe). The threshold curves measured following steady adaptation exhibit a steeper slope on the $+S$ side than the $-S$ side, replicating the results of Zaidi et al. (1992) and Krauskopf and Gegenfurtner (1992). The time-course of adaptation from $-S$ to W is slower than from $+S$ to W (similar to (Augenstein & Pugh, 1977; Stiles, 1949)). After $\pm S$ adaptation, the negative branch changes slope in a manner reminiscent of both branches in the RG color system, consistent with adaptation to the range of stimulation (Shapiro & Zaidi, 1992; Zaidi & Shapiro, 1993; Zaidi et al., 1998). The positive branch, on the other hand, does not change slope but shifts upwards, consistent with a multiplicative attenuation prior to the non-linearity (Shapiro & Zaidi, 1992; Zaidi & Shapiro, 1993). The independent nature of changes in the two lobes of the $\pm S$ curve can be seen more easily in Shapiro and Zaidi (1992).

In terms of adaptation to uniform fields, the Zaidi et al. (1992) model with pre-opponent multiplicative gain controls and a post-opponent response non-linearity predicts that the two lines ($+S$ and $-S$ w.r.t. A) relating probe thresholds versus flash magnitudes should have invariant slopes for all conditions. This strong prediction generally holds for all observers in W and $-S$ steady-state conditions and for measurements during the transition from $-S$ to W . This pattern can be contrasted with the shallower transitory curves for the $L-M$ system (Shapiro et al., 2000). For the $L-M$ system, it is possible that the shallowing effect is caused by a slower, higher-level adapting process (Zaidi et al., 1998). The transition from $-S$ to W has a slower time-course than the decay of higher-level adaptation to the $\pm S$ stimulus at this particular contrast level. Any higher-level effects are unlikely to be seen in the data.

There were some differences between the observers. For observer JLB, the transition from $-S$ to W took more time to settle than either the $+S$ to W , or the $\pm S$ to W . A fourth observer who ran only the $-S$ adaptation condition with a shorter re-adaptation period also produced a delay similar to that shown by observer JLB. The decrease in sensitivity immediately after $-S$ adaptation is similar to the phenomenon of transient tritanopia of the second kind (Mollon, Stockman, & Polden, 1987). Speculatively, the delay from $-S$ to W adaptation seen in our data may be related to the slow return to base level seen after cells are driven below their resting potential by biased input (Yeh, Lee, & Kremers, 1985). We have no theory concerning the nature of the individual differences.

The results from the $\pm S$ condition can eliminate a number of plausible mechanistic models of adaptation. (1) The data cannot be described by a simple multiplicative gain control placed before or after the non-linearity (see Shapiro & Zaidi, 1992, for algebraic analysis of these models). (2) The visual system is not simultaneously adapting to the two chromaticities that create the $\pm S$ stimulus, since the minimum of the thresholds for $-S$ and $+S$ adaptation are not similar to the $\pm S$ adaptation curve. (3) The data cannot be described by an integrator after the non-linearity coupled with multiplicative feedback to a site before the non-linearity. This type of mechanism will bring the signal back to W eventually. The signal will not rest at $-S$, as would be required to describe the $\pm S$ 0 s delay data. (4) The data cannot be described by subtracting a steady $-S$ signal from the flash signal. Such a model would predict large color shifts at W following $\pm S$ adaptation. Observers in this study did not report such color shifts, nor did Webster and Mollon (1994) report such a shift following sinusoidal contrast adaptation.

A fast higher-order adaptive response, such as we propose, differs from other models of the S -cone system that posit a fast adapting pre-opponent gain control followed by a slower post-opponent gain control (Augenstein & Pugh, 1977; Pugh & Mollon, 1979). While the effects of $\pm S$ adaptation cannot be explained entirely by a fast multiplicative gain control, it is conceivable that $\pm S$ adaptation affects a pre-opponent site on the positive branch and a post-opponent (higher-order) adaptive process on the negative branch. On the other hand, our conclusions are consistent with Loomis (1980) and Reeves (1981), who examined the effects of flickering lights on transient tritanopia. Loomis reported that recovery from square wave flickering lights was faster than recovery from steady adapting fields. In addition, both Loomis and Reeves ruled out a sluggish post-opponent integration system in the S -cone pathway. On the other hand, the $\pm S$ adaptation for observer LAB never returned completely to baseline after 1.0 s delay even though the initial recovery was faster than uniform field adaptation. This may represent a separate adaptation effect with a long persistence, such as the slow stage of chromatic adaptation proposed by Fairchild and Reniff (1995).

While it is likely that response to the $\pm S$ adaptation stimulus results in multiple sources of post-receptoral adaptation, a fast higher-order mechanism is physiologically plausible: Muller, Metha, Krauskopf, and Lennie (1999) have identified fast adaptive responses in cells in area V1. It is therefore conceivable that two types of post-opponent gain controls exist, a slow subtractive mechanism that arises under some steady adaptation conditions, and another fast higher-order mechanism that adapts to temporal changes. Additionally, there seem to be many different contrast adaptation

processes in retinal ganglion cells (Brown & Masland, 2001). Some of these processes take place on the order of 100 msec, while others occur on the order of seconds.

A fast higher-order adaptive process is also consistent with previous psychophysical reports. Zaidi et al. showed that static checker-board patterns can produce second-order chromatic adaptation, suggesting that the adaptive processes are fast enough to occur at the speed of eye-movements. Webster and Wilson (2000) and Shapiro, Hood, and Mollon (2003) showed that the maximum effect of 2nd order chromatic adaptation occurs when the rate of sinusoidal modulation is between 6 and 10 Hz. Shapiro, Hood and Mollon show that the adapting processes underlying contrast adaptation are not the same as those mediating chromatic sensitivity, which have a much slower temporal response. It is likely, although certainly not necessary, that the processes underlying the fast recovery from adaptation are the same as those that respond to fast sinusoidal modulation. These processes may or may not be related to those discussed by Greenlee, Georgeson, Magnussen, and Harris (1991), who measured the build up and decay of adaptation for achromatic gratings.

Unlike the gain-control model for adaptation to uniform fields, the fits of the regression lines to the *S*-cone contrast data are at best a data description. The changes are consistent with previous results (Shapiro & Zaidi, 1992; Zaidi & Shapiro, 1993). A simple characterization of adaptation to spatio-temporally variegated fields continues to elude us. The “response equalization” model (Zaidi & Shapiro, 1993) provides a qualitative explanation of the change in the negative branch. A related scheme proposed by MacLeod and von der Twer (1997) also provides the right trend for the negative branch. This class of adaptation is likely to be ubiquitous during active viewing of everyday scenes and as such is likely to be crucial to our understanding of how the visual system adapts to the natural environment.

Acknowledgements

This work was supported by NIH grants R15-EY12946 and EY07556.

References

- Augenstein, E. J., & Pugh, E. N. (1977). The dynamics of the π_1 color mechanism: further evidence for two sites of adaptation. *Journal of Physiology*, 272, 247–281.
- Brown, S. P., & Masland, R. H. (2001). Spatial Scale and cellular substrate of contrast adaptation by retinal ganglion cells. *Nature Neuroscience*, 4, 44–51.
- Burns, S. A., Elsner, A. E., Pokorny, J., & Smith, V. C. (1984). The Abney effect: chromaticity coordinates of unique and other constant hues. *Vision Research*, 24, 479–489.
- Craik, K. (1938). The effect of adaptation on differential brightness discrimination. *Journal of Physiology (London)*, 92, 406–421.
- Dacey, D. M. (2000). Parallel pathways for spectral coding in primate retina. *Annual Review of Neuroscience*, 23, 743–775.
- Derrington, A. M., Krauskopf, J., & Lennie, P. (1984). Chromatic mechanisms in lateral geniculate nucleus of macaque. *Journal of Physiology (London)*, 357, 241–265.
- Fairchild, M. D., & Reniff, L. (1995). Time-course of chromatic adaptation for color-appearance judgments. *Journal of the Optical Society of America A*, 12, 824–833.
- Geisler, W. S. (1978). Adaptation, afterimages and cone saturation. *Vision Research*, 18, 279–289.
- Greenlee, M. W., Georgeson, M. A., Magnussen, S., & Harris, J. P. (1991). The time course of adaptation to spatial contrast. *Vision Research*, 31, 223–236.
- Hayhoe, M. M., Benimoff, N. I., & Hood, D. C. (1987). The time-course of multiplicative and subtractive adaptation processes. *Vision Research*, 27, 1981–1996.
- Hendry, S. H. C., & Reid, R. C. (2000). The koniocellular pathway in primate vision. *Annual Review of Neuroscience*, 23, 127–153.
- Ikeda, M., & Ayama, M. (1980). Additivity of opponent chromatic valence. *Vision Research*, 20, 995–999.
- Krauskopf, J., & Gegenfurtner, K. (1992). Color discrimination and adaptation. *Vision Research*, 32, 2165–2175.
- Krauskopf, J., Williams, D. R., & Heeley, D. W. (1982). Cardinal directions of color space. *Vision Research*, 1123–1131.
- Krauskopf, J., Zaidi, Q., & Mandler, M. B. (1986). Mechanisms of simultaneous color induction. *Journal of the Optical Society of America A*, 3, 1752–1757.
- Larimer, J., Krantz, D. H., & Cicerone, C. M. (1975). Opponent process additivity II. Yellow/blue equilibria and nonlinear models. *Vision Research*, 15, 723–731.
- Loomis, J. (1980). Transient tritanopia: failure of time-intensity reciprocity in adaptation to longwave light. *Vision Research*, 20, 837–846.
- MacLeod, D. I. A., & Boynton, R. M. (1979). Chromaticity diagram showing cone excitation by stimuli of equal luminance. *Journal of the Optical Society of America A*, 69, 1183–1186.
- MacLeod, D. I. A., & von der Twer, T. (1997). Optimal nonlinear codes. *Investigative Ophthalmology and Vision Science*, 38(suppl.), S254.
- McLellan, J. S., & Eskew, R. T. (2000). ON and OFF *S*-cone pathways have different long-wave cone inputs. *Vision Research*, 40, 2449–2465.
- Mollon, J. D., Stockman, A., & Polden, P. G. (1987). Transient tritanopia of a second kind. *Vision Research*, 27, 637–650.
- Muller, J. R., Metha, A. B., Krauskopf, J., & Lennie, P. (1999). Rapid adaptation in visual cortex to the structure of images. *Science*, 285, 1405–1408.
- Pokorny, J., & Smith, V. C. (1997). Psychophysical signatures associated with magnocellular and parvocellular contrast gain control. *Journal of the Optical Society of America A*, 14, 2477–2486.
- Pugh, E. H., & Mollon, J. D. (1979). A theory of the π_1 and π_3 color mechanisms of Stiles. *Vision Research*, 19, 293–312.
- Reeves, A. (1981). Transient tritanopia after flicker adaptation. *Vision Research*, 21, 657–664.
- Shapiro, A. G., Baldwin, L. A., & Zaidi, Q. (2002). *Time course of L-M system adaptation to simple and complex fields*. Sarasota, FL: Visual Sciences Society.
- Shapiro, A. G., Beere, J. L., & Zaidi, Q. (2000). Time course of adaptation along the RG cardinal axis. *Color Research and Application*, 26, S43–S47.
- Shapiro, A. G., Pokorny, J., & Smith, V. C. (1996). Cone-rod receptor spaces with illustrations that use CRT phosphor and light-emitting-diode spectra. *Journal of the Optical Society of America*, 13, 2319–2328.

- Shapiro, A. G., & Zaidi, Q. (1992). The effects of prolonged temporal modulation on the differential response of color mechanisms. *Vision Research*, *32*, 2065–2075.
- Shapiro, A. G., Hood, S. M., Mollon, J. D. (2003). Temporal frequency and contrast adaptation. In: Mollon, J. D., Pokorny, J., Knoblauch, K. (Eds.), *Normal and defective colour vision*. Oxford University Press.
- Shapiro, A. G., Zaidi, Q., & Hood, D. (1990). Adaptation in the red–green (*L–M*) color system. *Investigative Ophthalmology and Vision Science*, *31*(suppl.), 262.
- Stiles, W. S. (1949). Increment thresholds and the mechanisms of colour vision. *Documenta Ophthalmologica*, *3*, 215–237.
- Valberg, A., Lee, B. B., & Tigwell, D. A. (1986). Neurones with strong inhibitory *S*-cone inputs in the macaque lateral geniculate nucleus. *Vision Research*, *26*, 1061–1064.
- von Wiegand, T. E., Hood, D. C., & Graham, N. (1995). Probed-sinewave paradigm: a test of models of light-adaptation dynamics. *Vision Research*, *35*, 3037–3051.
- Webster, M. A., & Mollon, J. D. (1991). Changes in colour appearance following post-receptor adaptation. *Nature*, *349*, 235–238.
- Webster, M. A., & Mollon, J. D. (1994). The influence of contrast adaptation on color appearance. *Vision Research*, *34*, 1993–2020.
- Webster, M. A., & Wilson, J. A. (2000). Interactions between chromatic adaptation and contrast adaptation in color appearance. *Vision Research*, *40*, 3801–3816.
- Wetherill, G. B., & Levitt, H. (1965). Sequential estimation of points on a psychometric function. *The British Journal of Mathematical and Statistical Psychology*, *18*, 1–10.
- Yeh, T., Lee, B. B., & Kremers, J. (1985). Temporal response of ganglion cells of the macaque retina to cone-specific modulation. *Journal of the Optical Society of America A*, *12*, 456–464.
- Yeh, T., Pokorny, J., & Smith, V. C. (1993). Chromatic discrimination with variation in chromaticity and luminance: data and theory. *Vision Research*, *33*, 1835–1845.
- Zaidi, Q., & Halevy, D. (1993). Visual mechanisms that signal the direction of color changes. *Vision Research*, *33*, 1037–1051.
- Zaidi, Q., & Shapiro, A. G. (1993). Adaptive orthogonalization of opponent-color signals. *Biological Cybernetics*, *69*, 415–428.
- Zaidi, Q., Shapiro, A. G., & Hood, D. (1992). The effects of adaptation on the differential sensitivity of the *S*-cone color system. *Vision Research*, *32*, 1297–1318.
- Zaidi, Q., Spehar, B., & DeBonet, J. (1998). Adaptation to textured chromatic fields. *Journal of the Optical Society of America A*, *15*, 23–32.